immunofluorescence photographs for phosphorylated FAK at Y397 and Y925 in conditions with or without TNC treatment. Larger and brighter focal adhesions were visible in the cells on TNC substrate. Bar, 20 μm. B: By immunoblotting, FAK phosphorylation at Y397 and Y925was determined. C: The graph shows the relative values of the phosphorylation to total FAK. TNC coating significantly enhanced FAK phosphorylation at both Y397 and Y925 after 10 min of PDGF-BB stimulation.

Fig. 6. TNC enhances SRC recruitment to αv integrin. A: Immunofluorescence of phosphorylated SRC at Y418 showed stronger labeling of the focal adhesions in TNC-treated cells after PDGF-BB stimulation. Bar, 20 μm. B: Cells were lysed with a lysis buffer, immunoprecipitated with αv subunit antibody (clone 21) and subjected to immunoblotting. Increased SRC was co-precipitated with integrin αv after PDGF-BB treatment. C: Furthermore, TNC treatment significantly increased the relative amount of SRC bound to integrin αv complex.

Figure 1

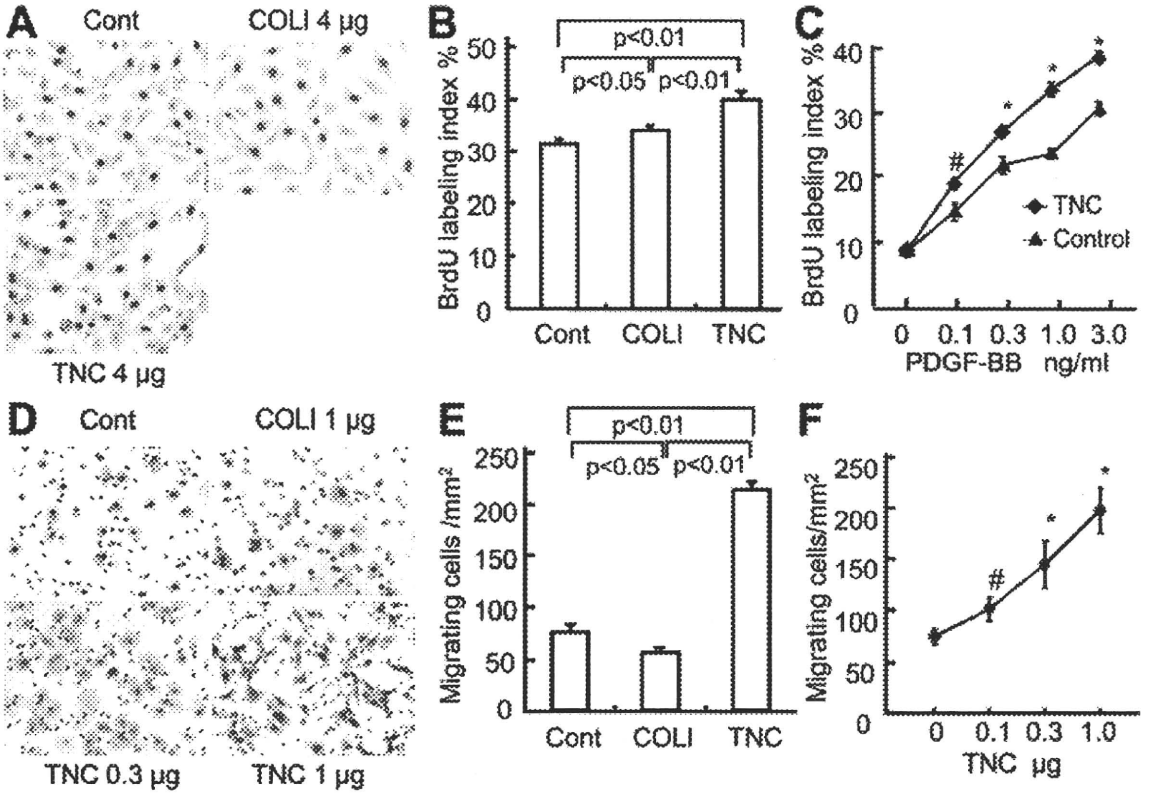

Figure 2

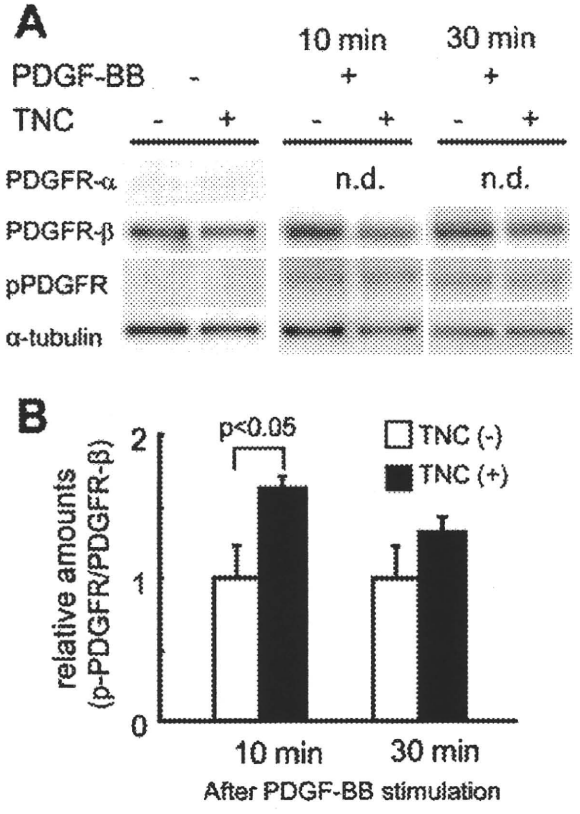

Figure 3

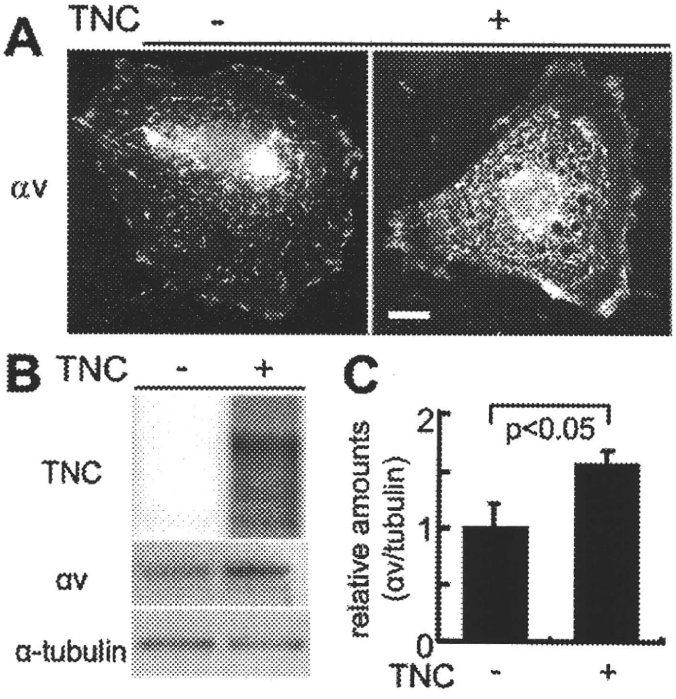

Figure 4

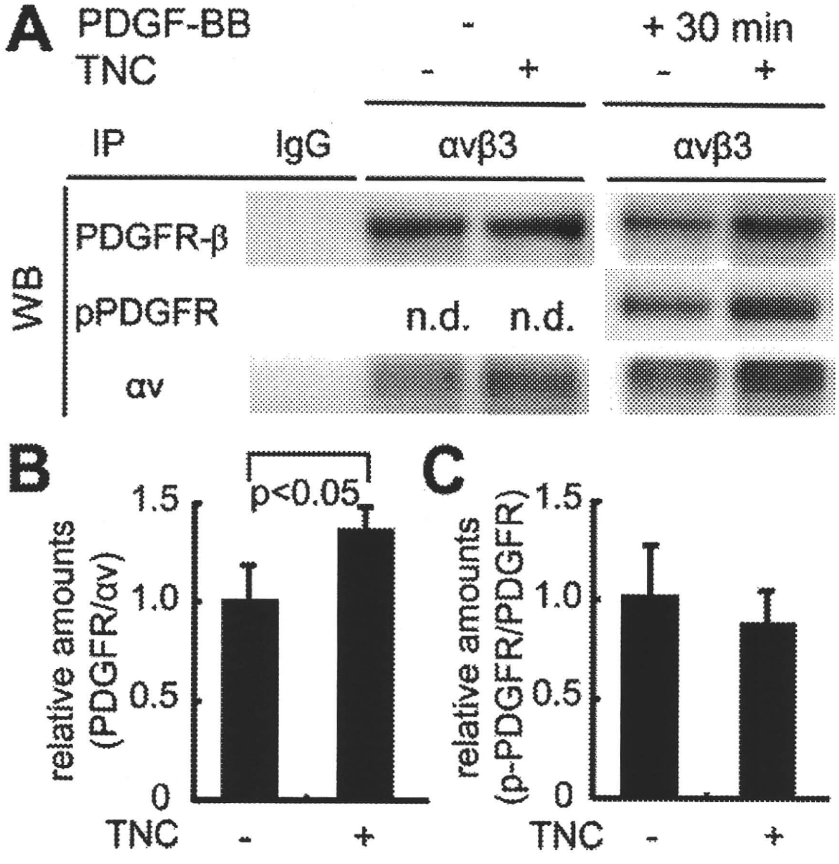

Figure 5

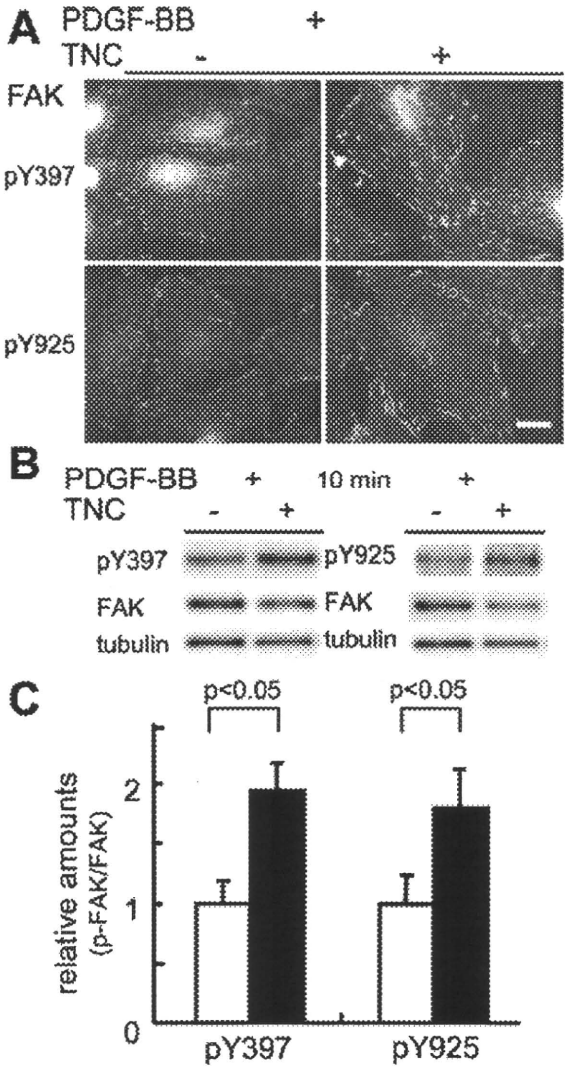

Figure 6

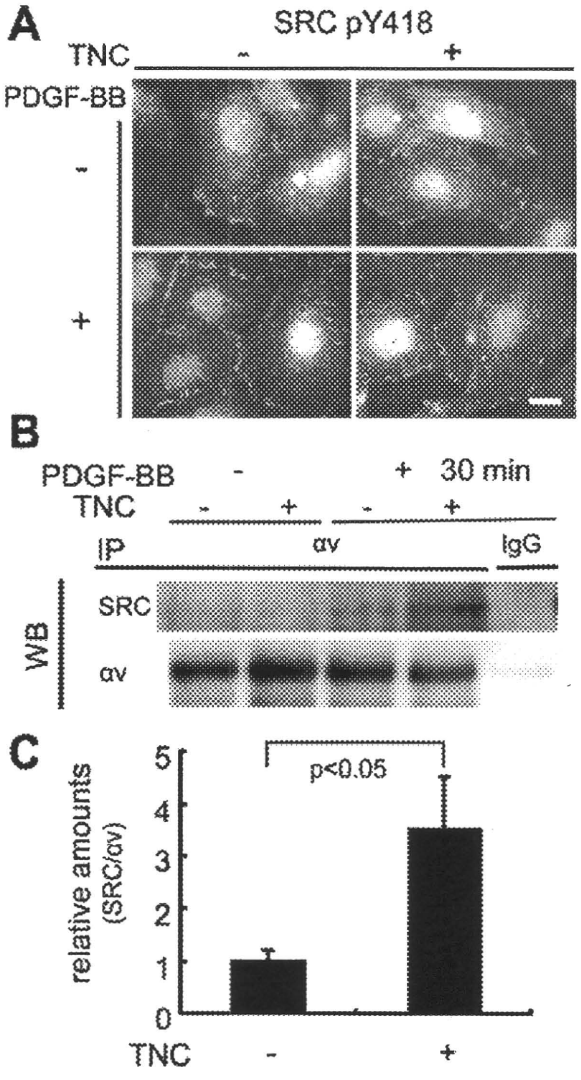

Autophagy 6:5, 600-606; July 1, 2010; © 2010 Landes Bioscience

Inhibition of autophagy in the heart induces age-related cardiomyopathy

Manabu Taneike,[1] Osamu Yamaguchi,[1] Atsuko Nakai,[2] Shungo Hikoso,[1] Toshihiro Takeda,[1] Isamu Mizote,[1] Takafumi Oka,[1] Takahito Tamai,[1] Jota Oyabu,[1] Tomokazu Murakawa,[1] Kazuhiko Nishida,[1] Takahiko Shimizu,[3] Masatsugu Hori,[1] Issei Komuro,[1] Takuji Shirasawa,[4] Noboru Mizushima[5] and Kinya Otsu[1,*]

[1]Department of Cardiovascular Medicine; Osaka University Graduate School of Medicine; Suita, Osaka Japan; [2]Chemical Biology Core Facility; Chemical Biology Department; Advanced Science Institute; RIKEN; Wako, Saitama Japan; [3]Department of Molecular Gerontology; Tokyo Metropolitan Institute of Gerontology; Tokyo, Japan; [4]Department of Aging Control Medicine; Juntendo University Graduate School of Medicine; Tokyo, Japan; and [5]Department of Physiology and Cell Biology; Tokyo Medical and Dental University; Tokyo, Japan

Key words: Atg5, autophagy, heart, aging, mitochondria

Abbreviations: *Atg*, autophagy-related; LC3, microtubule-associated protein 1 light chain 3; α-MyHC, α-myosin heavy chain; HNE, 4-hydroxy-2-nonenal

Constitutive autophagy is important for control of the quality of proteins and organelles to maintain cell function. Damaged proteins and organelles accumulate in aged organs. We have previously reported that cardiac-specific gene *Atg5* (autophagy-related 5)-deficient mice, in which the gene was floxed out early in embryogenesis, were born normally, and showed normal cardiac function and structure up to 10 weeks old. In the present study, to determine the longer-term consequences of *Atg5*-deficiency in the heart, we monitored cardiac-specific *Atg5*-deficient mice for an additional 12 months. First, we examined the age-associated changes of autophagy in the wild-type mouse heart. The level of autophagy, as indicated by decreased LC3-II (microtubule-associated protein 1 light chain 3-II) levels, in the hearts of 6-, 14- or 26-month-old mice was lower than that of 10-week-old mice. Next, we investigated the cardiac function and life span in cardiac-specific *Atg5*-deficient mice. The *Atg5*-deficient mice began to die after the age of six months. *Atg5*-deficient mice exhibited a significant increase in left ventricular dimension and decrease in fractional shortening of the left ventricle at the age of 10 months, compared to control mice, while they showed similar chamber size and contractile function at the age of three months. Ultrastructural analysis revealed a disorganized sarcomere structure and collapsed mitochondria in 3- and 10-month-old *Atg5*-deficient mice, with decreased mitochondrial respiratory functions. These results suggest that continuous constitutive autophagy plays a crucial role in maintaining cardiac structure and function.

Introduction

In developed countries, heart failure is one of the major causes of death, and novel effective therapies are needed for patients that experience this disease. Heart failure is an age-related disease and the incidence increases with age.[1] Increasing age causes a progressive, functional impairment of tissues and organs and enhances their vulnerability to stress. Damage to proteins, membrane lipids, DNA and cellular organelles plays an important role in aging.[2,3] The accumulation of damaged proteins and organelles, such as mitochondria, accounts for the age-associated malfunction of many biological processes. Reduced degradation of proteins and organelles may contribute to their accumulation and to the aging process.[4] The ubiquitin/proteasome and autophagy systems are two major proteolytic systems. Autophagy is a cellular process that degrades long-lived proteins and recycles components.[5] The age-associated reduction of autophagic activity has been reported.[4,6] Autophagy-related genes are required for life-span extension in various long-lived mutant nematodes, and they promote survival in worms and flies exposed to prolonged starvation.[7] Furthermore, promotion of expression of the autophagy gene, *Atg8*, in the nervous system of Drosophila extends its life span.[8] These data implicate autophagy in aging.

We previously reported on the role of autophagy, using cardiac-specific *Atg5*-deficient mice.[9] Atg5 is an essential protein for autophagy.[10] Atg5, conjugated with Atg12, is required for elongation of the phagophore to form an autophagosome, and also for targeting of Atg8 to the phagophore membrane. When the *Atg5* gene is floxed out in adulthood, *Atg5*-deficient mice show left ventricular dilation and contractile dysfunction. On the other hand, when the *Atg5* gene is floxed out early in embryogenesis, the mice show no cardiac phenotypes under baseline conditions up to 10 weeks of age. In this study, we attempted to determine

*Correspondence to: Kinya Otsu; Email: kotsu@medone.med.osaka-u.ac.jp
Submitted: 01/18/10; Revised: 03/31/10; Accepted: 04/01/10
Previously published online: www.landesbioscience.com/journals/autophagy/article/11947

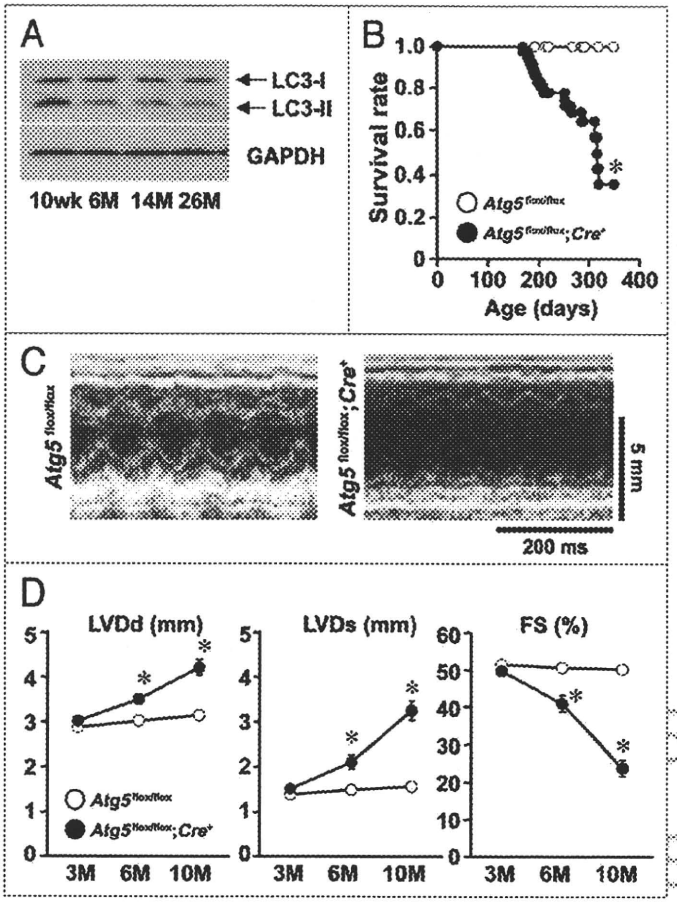

Figure 1. Alteration of autophagic activity in aging in wild-type mouse hearts and characterization of cardiac-specific *Atg5*-deficient mice. (A) Western blotting analysis of LC3 in the heart of wild-type C57Bl/6J mice. A representative blot is shown. (B) Survival curve for *Atg5*$^{flox/flox}$;α-MyHC-*Cre*$^{-}$ (*Atg5*$^{flox/flox}$) and *Atg5*$^{flox/flox}$;α-MyHC-*Cre*$^{+}$ (*Atg5*$^{flox/flox}$;*Cre*$^{+}$) mice. (C and D) Trans-thoracic M-mode echocardiographic analyses. Representative images of tracings are shown in (C). Echocardiographic measurements are shown in (D). LVDd, diastolic left ventricle internal dimension; LVDs, systolic left ventricle internal dimension; FS, fractional shortening of left ventricle dimension. Values represent the mean ± s.e.m. of data from 11 to 24 mice in each group. *$p < 0.05$ versus corresponding group.

the longer-term consequences of Atg5-deficiency in the heart. Our results suggest that constitutive continuous autophagy plays an important role to maintain cardiac structure and function.

Results

We first attempted to evaluate the alteration of autophagic activity in the heart brought about by aging. We performed western blotting analysis of LC3, which has been used as a molecular marker of autophagic activity. The conversion of LC3-I to LC3-II is an essential step during autophagosome formation. The protein level of LC3-II in homogenates prepared from the hearts of 6-, 14- or 26-month-old wild-type C57Bl/6J mice was lower than that from the hearts of 10-week-old mice (**Fig. 1A**). This suggests that the level of autophagy in the heart decreases with increasing age, in agreement with previous reports.[4,6,11,12]

In order to elucidate the role of autophagy in the heart, we generated cardiac-specific *Atg5*-deficient mice. We crossed mice bearing a floxed *Atg5* allele with transgenic mice expressing *Cre* recombinase under the control of α-myosin heavy chain promoter (α-MyHC-*Cre*), to produce *Atg5*$^{flox/flox}$;α-MyHC-*Cre*$^{+}$ mice. In these mice, the *Atg5* gene was floxed early in embryogenesis. The cardiac-specific *Atg5*-deficient mice were born normally and exhibited no cardiac abnormalities at 10 weeks of age;[9] we used *Atg5*$^{flox/flox}$;α-MyHC-*Cre*$^{-}$ littermates as controls. We next evaluated the survival rate of the *Atg5*$^{flox/flox}$;α-MyHC-*Cre*$^{+}$ mice (**Fig. 1B**). These mice started to die at 6 months of age, and the median life span was approximately one year, while no *Atg5*$^{flox/flox}$;α-MyHC-*Cre*$^{-}$ mice died within one year. We also evaluated physiological parameters in 3- and 10-month-old *Atg5*$^{flox/flox}$;α-MyHC-*Cre*$^{+}$ mice (**Table 1**). There were no significant differences in body weight, heart weight, lung weight or liver weight between *Atg5*$^{flox/flox}$;α-MyHC-*Cre*$^{+}$ and *Atg5*$^{flox/flox}$;α-MyHC-*Cre*$^{-}$ mice at 3 months of age. The heart weight, lung weight, the ratio of whole heart weight to tibia length, and the ratio of lung weight to tibia length were significantly higher in *Atg5*$^{flox/flox}$;α-MyHC-*Cre*$^{+}$ mice at 10 months. There were no significant differences in body weight, liver weight or tibia length between *Atg5*$^{flox/flox}$;α-MyHC-*Cre*$^{+}$ and *Atg5*$^{flox/flox}$;α-MyHC-*Cre*$^{-}$ mice at 10 months of age.

We used trans-thoracic M-mode echocardiographic analysis to evaluate changes in the cardiac function of *Atg5*-deficient mice with increasing age (**Table 2, Fig. 1C and D**). Representative images of tracings indicate that 10-month-old *Atg5*$^{flox/flox}$;α-MyHC-*Cre*$^{+}$ mice showed chamber dilatation compared with *Atg5*$^{flox/flox}$;α-MyHC-*Cre*$^{-}$ mice (**Fig. 1C**). There were no differences in the end-diastolic and end-systolic left ventricular internal dimensions or fractional shortening between *Atg5*$^{flox/flox}$;α-MyHC-*Cre*$^{+}$ and *Atg5*$^{flox/flox}$;α-MyHC-*Cre*$^{-}$ mice at three months of age. However, the end-diastolic and end-systolic left ventricular internal dimensions of 6- and 10-month-old *Atg5*$^{flox/flox}$;α-MyHC-*Cre*$^{+}$ mice were significantly larger than the corresponding controls. Furthermore, fractional shortening of the *Atg5*$^{flox/flox}$;α-MyHC-*Cre*$^{+}$ mice was significantly lower than that of the corresponding controls.

The hearts of 10-month-old *Atg5*$^{flox/flox}$;α-MyHC-*Cre*$^{+}$ mice showed chamber dilatation compared with *Atg5*$^{flox/flox}$;α-MyHC-*Cre*$^{-}$ mice, in agreement with echocardiographic analysis (**Fig. 2A**). The *Atg5*$^{flox/flox}$;α-MyHC-*Cre*$^{+}$ mice showed a significant increase in the cross-sectional area of cardiomyocytes, compared to the control mice (**Fig. 2A and B**). Furthermore, Mallory-Azan staining indicated that *Atg5*$^{flox/flox}$;α-MyHC-*Cre*$^{+}$ mouse hearts had enhanced intercellular and peri-vascular fibrosis (**Fig. 2A**). In agreement with the histological analysis, the mRNA level of collagen type 1 (*Col1a2*) in *Atg5*$^{flox/flox}$;α-MyHC-*Cre*$^{+}$ mouse hearts was higher than that in controls. We observed higher levels of the mRNA expression of molecular markers for cardiac remodeling,

Table 1. Physiological parameters of cardiac-specific *Atg5*-deficient mice at 3 or 10 months of age

	3-month-old		10-month-old	
	$Atg5^{flox/flox}$	$Atg5^{flox/flox}$; Cre^+	$Atg5^{flox/flox}$	$Atg5^{flox/flox}$; Cre^+
BW (g)	25.9 ± 0.12	27.8 ± 1.88	32.1 ± 0.76	33.2 ± 1.16
HW (mg)	135.0 ± 8.92	134.9 ± 12.55	158.0 ± 4.15	180.9 ± 5.22*
Lung (mg)	121.7 ± 5.95	124.0 ± 7.29	136.9 ± 2.63	153.3 ± 5.76*
Liver (mg)	1280.6 ± 195.33	1414.5 ± 130.87	1269.8 ± 78.25	1328.8 ± 108.31
Tibia (mm)	17.9 ± 0.12	18.2 ± 0.13	18.1 ± 0.13	18.3 ± 0.12
HW/BW (mg/g)	5.21 ± 0.368	4.84 ± 0.135	4.96 ± 0.180	5.52 ± 0.212
HW/Tibia (mg/mm)	7.52 ± 0.479	7.40 ± 0.643	8.72 ± 0.260	9.88 ± 0.289*
Lung/BW (mg/g)	4.69 ± 0.250	4.49 ± 0.339	4.28 ± 0.087	4.65 ± 0.173
Lung/Tibia (mg/mm)	6.78 ± 0.291	6.80 ± 0.379	7.55 ± 0.145	8.37 ± 0.304*

$Atg5^{flox/flox}$, *Atg5*$^{flox/flox}$; α-MyHC-*Cre*$^-$; $Atg5^{flox/flox}$; Cre^+, *Atg5*$^{flox/flox}$; α-MyHC-*Cre*$^+$; BW, body weight; HW, whole heart weight; HW/BW, whole heart-to-body weight ratio; HW/Tibia, whole heart weight-to-tibia length ratio; Lung/BW, lung-to-body weight ratio; Lung/Tibia, lung weight-to tibia length ratio. Values represent the mean ± s.e.m. of data from 3 to 15 mice in each group. *$p < 0.05$ versus corresponding group.

Table 2. Echocardiographic parameters of cardiac-specific *Atg5*-deficient mice at 3 or 10 months of age

	3-month-old		10-month-old	
	$Atg5^{flox/flox}$	$Atg5^{flox/flox}$; Cre^+	$Atg5^{flox/flox}$	$Atg5^{flox/flox}$; Cre^+
LVDd (mm)	2.88 ± 0.04	3.02 ± 0.07	3.13 ± 0.07	4.21 ± 0.17*
LVDs (mm)	1.40 ± 0.03	1.51 ± 0.05	1.56 ± 0.05	3.24 ± 0.22*
IVSd (mm)	0.88 ± 0.02	0.94 ± 0.02	0.97 ± 0.03	0.77 ± 0.04*
LVPWd (mm)	0.83 ± 0.02	0.82 ± 0.04	0.81 ± 0.03	0.69 ± 0.04*
FS (%)	51.4 ± 0.63	49.8 ± 0.98	50.2 ± 0.86	23.7 ± 2.20*
Heart rate (bpm)	726 ± 7.3	705 ± 10.4	707 ± 11.3	674 ± 11.5

LVDd, diastolic left ventricle internal dimension; LVDs, systolic left ventricle internal dimension; IVSd, diastolic interventricle septal wall thickness; LVPWd, diastolic left ventricle posterior wall thickness; FS, fractional shortening of left ventricle dimension. Values represent the mean ± s.e.m. of data from 11 to 17 mice in each group. *$p < 0.05$ versus corresponding group.

such as atrial natriuretic factor (*Nppa*), brain natriuretic peptide (*Nppb*) and skeletal α-actin (*Acta1*) mRNAs (**Fig. 2C**), in *Atg5*$^{flox/flox}$;α-MyHC-*Cre*$^+$ mouse hearts. Thus, *Atg5*$^{flox/flox}$;α-MyHC-*Cre*$^+$ mice showed contractile dysfunction and heart failure at 10 months of age.

We examined the levels of polyubiquitinated proteins, p62 and proteasome activity in *Atg5*$^{flox/flox}$;α-MyHC-*Cre*$^+$ mouse hearts (**Fig. 3**). The levels of polyubiquitinated proteins and p62 were increased in *Atg5*$^{flox/flox}$;α-MyHC-*Cre*$^+$ mouse hearts (**Fig. 3A**). We observed no significant difference in the proteasome activity between *Atg5*$^{flox/flox}$;α-MyHC-*Cre*$^+$ mouse hearts and controls (**Fig. 3B**).

We also performed ultrastructural analysis using electron microscopy. The hearts of 10-month-old *Atg5*$^{flox/flox}$;α-MyHC-*Cre*$^+$ mice showed dysalignment, aggregation and variety in the size of mitochondria (**Fig. 4A**), and the intramitochondrial structure was destroyed, as shown in the subpanel. To elucidate the cause of cardiac remodeling in aged *Atg5*$^{flox/flox}$;α-MyHC-*Cre*$^+$ mice, we performed ultrastructural analysis on the hearts of 3-month-old *Atg5*$^{flox/flox}$;α-MyHC-*Cre*$^+$ mice. Although the mice did not exhibit cardiac dysfunction at three months of age, the hearts already showed the abnormality of the mitochondria similar to that of the 10-month-old *Atg5*$^{flox/flox}$;α-MyHC-*Cre*$^+$ mouse hearts.

To evaluate the functional effect of the mitochondrial abnormalities, we measured the respiratory chain enzyme activities of mitochondria in the hearts of 3-month-old *Atg5*$^{flox/flox}$;α-MyHC-*Cre*$^+$ mice (**Fig. 4B**). The activities of both complex I + III and complex II + III in the hearts of *Atg5*$^{flox/flox}$;α-MyHC-*Cre*$^+$ mice were significantly decreased, compared with those in *Atg5*$^{flox/flox}$;α-MyHC-*Cre*$^-$ mice. Next, we measured the level of heme oxygenase-1 mRNA, which is an oxidative marker,[13] using real-time PCR (**Fig. 4C**). The expression level of heme oxygenase-1 mRNA in *Atg5*$^{flox/flox}$;α-MyHC-*Cre*$^+$ mouse hearts was higher than that in *Atg5*$^{flox/flox}$;α-MyHC-*Cre*$^-$ mouse hearts at three months of age. Furthermore, we performed western blotting analysis of 4-hydroxy-2-nonenal (HNE) adduct proteins in the mitochondrial fraction of the heart to confirm the increase in oxidative stress in *Atg5*$^{flox/flox}$;α-MyHC-*Cre*$^+$ mouse hearts (**Fig. 4D**), and showed that the increase of adduct proteins did occur. Then, we evaluated the level of cardiomyocyte apoptosis using the TUNEL assay (**Fig. 4E**). The number of TUNEL-positive cardiomyocytes in *Atg5*$^{flox/flox}$;α-MyHC-*Cre*$^+$ mouse hearts was higher than that in *Atg5*$^{flox/flox}$;α-MyHC-*Cre*$^-$ mouse hearts at 3 months of age. The TUNEL-positive cells were α-sarcomeric actin-positive, indicating that these were cardiomyocytes.

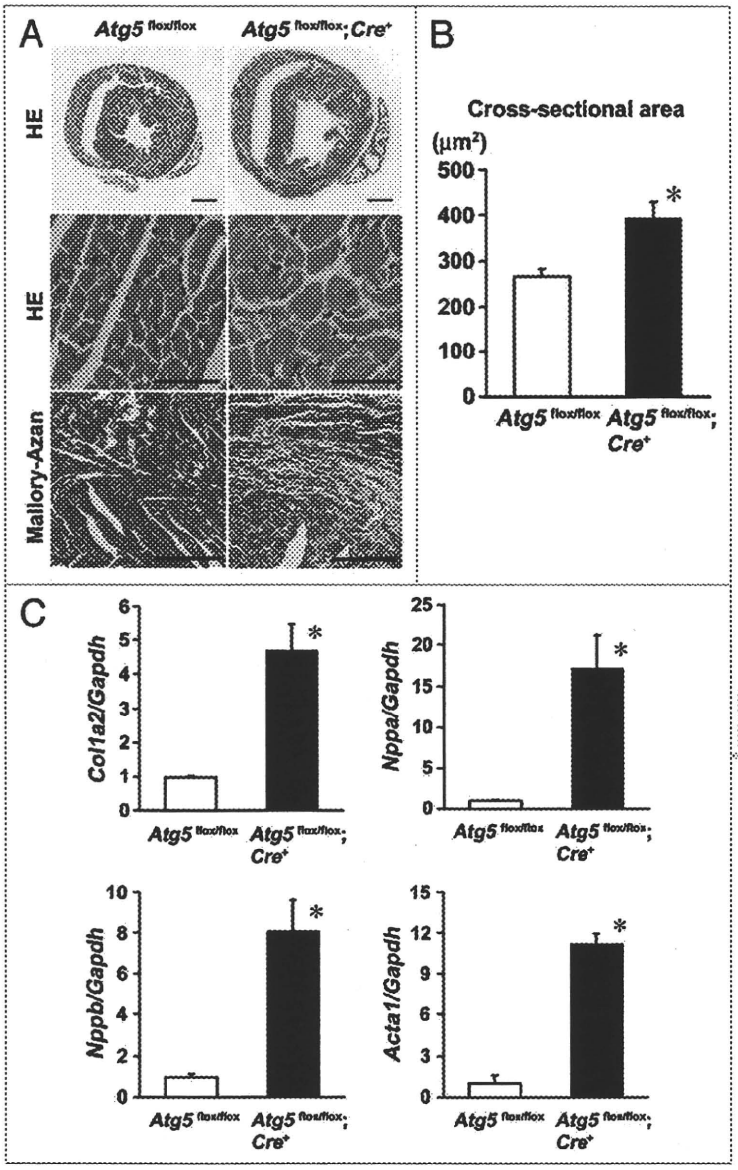

Figure 2. Age-related responses in 10-month-old cardiac-specific *Atg5*-deficient mice. (A) Histological analyses on the hearts of *Atg5*$^{flox/flox}$;α-MyHC-*Cre* (*Atg5*$^{flox/flox}$) and *Atg5*$^{flox/flox}$;α-MyHC-*Cre*$^{+}$ (*Atg5*$^{flox/flox}$;*Cre*$^{+}$) mice. Top panels, macroscopic hematoxylin-eosin (HE)-stained sections of hearts. Middle and bottom panels, microscopic HE-stained and Mallory-Azan-stained sections of left ventricle, respectively. (B) Cross-sectional area of cardiomyocytes. These were measured by tracing the outline of 100 myocytes in each section. Values represent the mean ± s.e.m. of data from 3 mice in each group. (C) Effect of Atg5 deficiency on *Col1a2*, *Nppa*, *Nppb* and *Acta1* mRNA expression. mRNA levels were determined by quantitative RT-PCR. Data were normalized to the *Gapdh* content and are expressed as fold increase over levels in the *Atg5*$^{flox/flox}$ group. Values represent the mean ± s.e.m. of data from 3 to 8 mice in each group. *$p < 0.05$ versus another group. Scale bars in (A): 1 mm in HE-stained macroscopic images; 50 μm in HE-stained microscopic images; 200 μm in Mallory-Azan-stained images.

Discussion

In the present study, we showed that cardiac-specific *Atg5* ablation led to chamber dilatation and cardiac dysfunction with increasing age. Cardiac-specific *Atg5*-deficient mouse hearts showed no cardiac phenotypes at three months of age. Some compensatory mechanisms prevented the pathological consequences of autophagy inhibition. Such mechanisms will involve Atg5-independent autophagy and chaperone-mediated autophagy.[4,14] In addition, mitochondria are continuously remodeled by fusion and fission.[15] Mitochondrial fusion and fission is a mechanism to maintain normal functional mitochondria. However, it remains to identify the compensatory mechanisms.

It has been reported that cardiac-specific overexpression of a protein led to apoptosis and cardiomyopathy with increasing age.[16] To exclude the possibility that overexpressed Cre protein led to the cardiac abnormalities observed in the present study, we evaluated *Atg5*-deficient mice in which *Cre* was knocked-in downstream of the myosin light chain 2v promoter. The resulting mice exhibited phenotypes similar to *Atg5*$^{flox/flox}$;α-MyHC-*Cre*$^{+}$ mice (data not shown). Furthermore, α-MyHC-*Cre*$^{+}$ mice exhibited similar cardiac function to their control non-transgenic mice up to 12 months of age (data not shown). These results suggest that the efficiency of the compensatory mechanisms is not sufficient enough to eliminate damaged proteins and organelles and to maintain cardiac function for a long time period, and that basal continuous Atg5-dependent autophagy is required to maintain cardiac structure and function.

We observed increases in accumulation of polyubiquitinated proteins and p62, and structural and functional abnormalities in mitochondria in *Atg5*-deficient hearts. Failure to turn over organelles and toxic proteins leads to their accumulation and functional abnormalities. The accumulation of dysfunctional organelles and toxic proteins in cardiomyocytes may result in global cardiac dysfunction.

We observed structural and functional abnormalities of the mitochondria in 3-month-old *Atg5*-deficient hearts, when we did not yet observe cardiac dysfunction. The mitochondrial abnormalities could not, therefore, be the result of age-related cardiomyopathy, but could be a cause of it. Mitochondria in aged post-mitotic cells are enlarged and structurally deteriorated, showing swelling and loss of cristae, and are deficient in ATP production.[17,18] These senescent-like abnormalities of mitochondria in autophagy-deficient cardiomyocytes might be responsible for cardiac dysfunction at 10 months of age.

Mitochondrial activity is a major source of endogenous reactive oxygen species (ROS) causing oxidative

damage of cytosolic materials.[19] We detected increases in the levels of heme oxygenase-1 mRNA and HNE adduct proteins and the number of apoptotic cardiomyocytes in 3-month-old *Atg5*$^{flox/flox}$;α-MyHC-*Cre*$^{+}$ mouse hearts. Increased oxidative stress in the heart can lead to cardiomyopathy.[20-22] It is possible that the accumulation of abnormal mitochondria results in increased oxidative stress, leading to cardiomyocyte apoptosis.

It has been reported that autophagy plays a pivotal role in aging.[7] We observed that the protein level of LC3-II in heart homogenates from 6-, 14- or 26-month-old mice was lower than that from 10-week-old mice. This suggests that the autophagic activity in the heart decreases with aging, in agreement with previous reports.[4,6,11,12] Although one has to measure autophagy flux to conclude age-associated reduction of autophagic activity, it is difficult to measure the flux in vivo. Cellular senescence is associated with typical phenotypic changes, such as an increase in senescence-associated β-galactosidase activity and cell cycle inhibitors such as p16 and p19.[23] Some of the phenotypic alterations have also been observed in animal tissues. In addition, lipofuscin, an autofluorescent, nondegradable and polymeric substance composed of cross-linked protein and lipid residues, is thought to be generated from damaged protein.[4] Aged postmitotic cells such as cardiac myocytes and neurons accumulate a large amount of lipofuscin. We evaluated senescence markers for aging in *Atg5*$^{flox/flox}$;α-MyHC-*Cre*$^{+}$ mouse hearts (data not shown). We could not detect cells positive for senescence-associated β-gal activity in 3- or 10-month-old *Atg5*$^{flox/flox}$;α-MyHC-*Cre*$^{+}$ mice or control mice. The protein level of p16 was increased in 3-month-old *Atg5*$^{flox/flox}$;α-MyHC-*Cre*$^{+}$ mice, compared to controls. We found no differences in the amount of lipofuscin between *Atg5*$^{flox/flox}$;α-MyHC-*Cre*$^{+}$ and control mice at 3 or 10 months of age. Although the inhibition of autophagy is not directly related to all features of senescence, reduction of autophagy during aging may be one of the causes of age-related cardiac dysfunction. Aging is a multifactorial process, with many mechanisms contributing to functional decline in organs and tissues.

In conclusion, we reported here that cardiac-specific *Atg5*-deficient mice showed age-related cardiomyopathy. Continuous constitutive autophagy plays an important role in maintaining cardiac structure and function. Thus, upregulation of autophagy might be a therapeutic target for the prevention of age-related cardiac dysfunction.

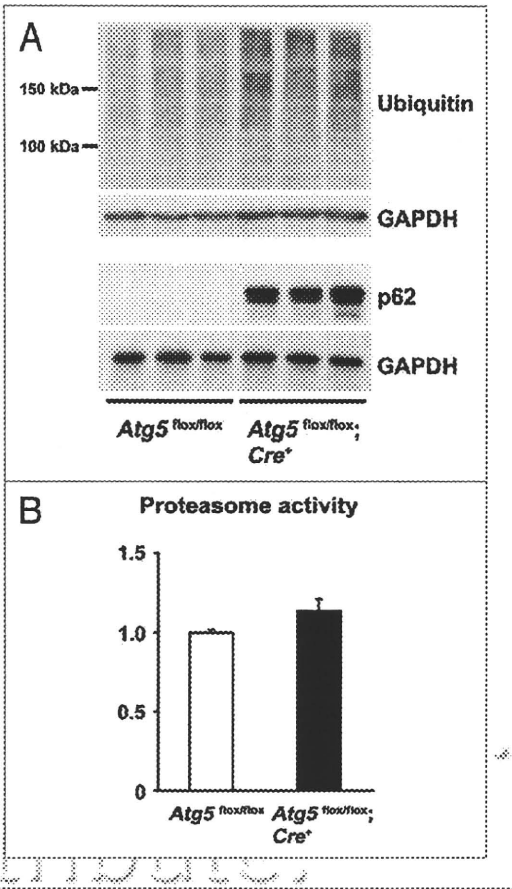

Figure 3. Protein accumulation in 10-month-old *Atg5*-deficient hearts. (A) Western blot analysis of ubiquitin and p62 in the hearts of *Atg5*$^{flox/flox}$;α-MyHC-*Cre* (*Atg5*$^{flox/flox}$) and *Atg5*$^{flox/flox}$;α-MyHC-*Cre*$^{+}$ (*Atg5*$^{flox/flox}$;*Cre*$^{+}$) mice. (B) Proteasome activity. Data are expressed as fold increase over the level in the *Atg5*$^{flox/flox}$ group. Values represent the mean ± s.e.m. of data from 3 to 4 mice in each group.

Materials and Methods

Mice and in vivo assessment of cardiac function. The generation of mice bearing an *Atg5*^{flox} allele, in which exon 3 of the *Atg5* gene is flanked by two loxP sequences, has been previously reported.[5] Mice bearing an *Atg5*^{flox} allele were crossed with transgenic mice expressing *Cre* recombinase under the control of α-myosin heavy chain promoter (α-MyHC-*Cre*).[24] The mice were maintained individually and allowed access to water and mouse chow ad libitum. To perform echocardiography on unsedated mice, we used ultra-sonography (SONOS-5500, equipped with a 15-MHz linear transducer, Philips Medical Systems). This study was carried out under the supervision of the Animal Research Committee of Osaka University and in accordance with the Guidelines for Animal Experiments of Osaka University and the Japanese Animal Protection and Management Law (No. 25).

Antibodies. The following antibodies were used for the western blotting analysis: mouse monoclonal GAPDH-specific antibody (Abcam, ab9482), rabbit ubiquitin-specific polyclonal antibody (DakoCytomation, Z0458), guinea pig p62-specific (C-terminal-specific) polyclonal antibody (Progen, GP62-C), rabbit NHE Michael Adducts-specific polyclonal antibody (Calbiochem, 393207), mouse COX IV-specific monoclonal antibody (Abcam, ab33985) and antibody to LC3.[25] Tissues were lysed in a homogenization buffer (50 mM Tris-HCl (Sigma, T1503), pH 7.4, 1 mM EDTA (Wako, 345-01865), 1 mM EGTA (Wako, 346-01312), 1% Triton X-100 (Wako 168-11805)) with proteinase inhibitors (PMSF (Wako, 160-12183), Leupeptin (Wako, 126-03754)). Western blots were developed with the ECL Plus kit (Amersham Biosciences Corp., RPN2132) or ECL Advance kit (Amersham Biosciences Corp., RPN2135).

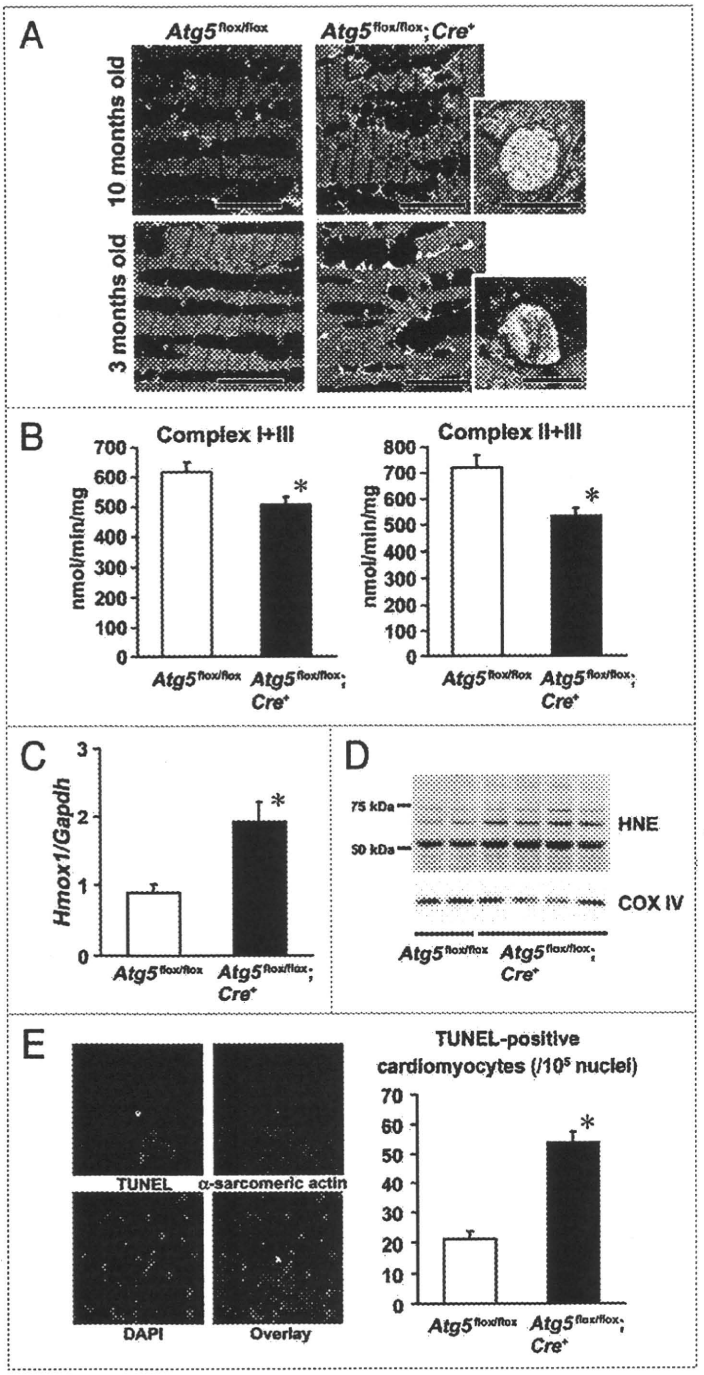

Figure 4. Histological and biochemical abnormalities in mitochondria of *Atg5*-deficient hearts. (A) Electron micrographs of 10- and 3-month-old *Atg5*$^{flox/flox}$;α-MyHC-*Cre* (*Atg5*$^{flox/flox}$) and *Atg5*$^{flox/flox}$;α-MyHC-*Cre*$^{+}$ (*Atg5*$^{flox/flox}$;*Cre*$^{+}$) mouse hearts. Intramitochondrial structure is shown in the subpanels. (B) The activities of complex I + III and complex II + III in mitochondria. Values represent the mean ± s.e.m. of data from 6 to 8 mice in each group. (C) The expression level of *Hmox1* mRNA determined by quantitative RT-PCR. Data were normalized to the *Gapdh* content and are expressed as fold increase over the level in the *Atg5*$^{flox/flox}$;α-MyHC-*Cre* group. Values represent the mean ± s.e.m. of data from 5 to 9 mice in each group. (D) Western blot analysis of HNE adduct proteins in the mitochondrial fraction from the heart. (E) Left, representative confocal images of the TUNEL-positive cardiomyocytes. Triple staining (TUNEL, α-sarcomeric actin and DAPI) was performed. Staining for TUNEL is shown in green, that for α-sarcomeric actin-specific antibody in red and that for DAPI in blue. In the overlay image, a nucleus stained by both TUNEL and DAPI is shown in blue-green. Right, the number of TUNEL-positive cardiomyocytes. Values represent the mean ± s.e.m. of data from 3 mice in each group. *$p < 0.05$ versus another group. Scale bars: 5 μm in (A); 1 μm in subpanels of (A).

Histological analysis. The hearts were excised and immediately fixed in buffered 4% paraformaldehyde (Wako, 162-16065), embedded in paraffin, and sectioned to a thickness of 3 μm. We performed hematoxylin-eosin or Mallory-Azan staining on serial sections. For electron microscopy, the hearts were fixed with 2.5% glutaraldehyde (Wako, 071-02031) in PBS. To determine the number of cells undergoing nuclear fragmentation, we performed a TUNEL assay on paraffin-embedded heart sections, using an in situ apoptosis detection kit (Takara Bio Inc., MK500).

Quantitative real-time reverse transcriptase-PCR (RT-PCR). We isolated total RNA from the left ventricle for analysis using the TRIzol reagent (Invitrogen Life Technologies, 15596-026). We determined mRNA levels for *Nppa, Nppb, collagen type 1 alpha2 (Col1a2), skeletal α-actin (Acta1), heme oxygenase-1 (Hmox1)* and *Gapdh* by quantitative RT-PCR. For reverse transcription and amplification, we used the TaqMan Reverse Transcription Reagents (Applied Biosystems, N808-0234) and Platinum Quantitative PCR SuperMix-UDG (Invitrogen Life Technologies, 11730-025), respectively. The PCR primers and probes of *Nppa* (Assay ID: Mm01255747_g1), *Nppb* (Assay ID: Mm00435304_g1), *Col1a2* (Assay ID: Mm01165187_m1), *Acta1* (Assay ID: Mm00808218_g1) and *Gapdh* (4352339E) were obtained from Applied Biosystems. The PCR primers and probe of *Hmox1* were designed as follows: forward primer GCC TCA CTG GCA GGA AAT CA, reverse primer GGA GAC GCT TTA CAT AGT GCT GTG T and probe CCT TGC ACG CCA GC. We constructed RT-PCR standard curves using the corresponding cDNA. All data were normalized to *Gapdh* content and are expressed as fold increase over the control group.

Proteasome activity analysis. We evaluated proteasome activity in homogenates of hearts using the 20S Proteasome Activity Assay Kit (Chemicon, APT280).

Mitochondrial enzyme activities. The activities of NADH-cytochrome-*c* oxidoreductase (complex I + III) and succinate-cytochrome-*c* oxidoreductase (complex II + III) were determined in mitochondrial fractions from hearts using previously described spectrophotometric methods.[26] Results are shown as nmol/min/mg protein.

Statistical analysis. Results are shown as the mean ± s.e.m. Paired data were evaluated using the Student's t-test. The Kaplan-Meier method with Logrank test was used for survival analysis. A value of $p < 0.05$ was considered statistically significant.

Acknowledgements

We thank Dr. Kenneth R. Chien, Harvard University for the generous gift of the myosin light chain 2v promoter-driven *Cre* knock-in mice and Dr. Tamotsu Yoshimori, Osaka University for antibody to LC3. This work was supported by a Grant-in-Aid for Scientific Research from the Ministry of Education, Culture, Sports, Science and Technology, Japan and by Takeda Medical Research Foundation to K. Otsu.

References

1. Schwartz JB, Zipes DP. Cardiovascular disease in the elderly. In: Libby P, Bonow RO, Mann DL, Zipes DP, eds. Braunwald's Heart Disease: A textbook of cardiovascular medicine. 8th edition. Philadelphia, PA: Elsevier 2008; 1923-53.
2. Martin GM, Austad SN, Johnson TE. Genetic analysis of ageing: role of oxidative damage and environmental stresses. Nat Genet 1996; 13:25-34.
3. Stadtman E. Protein oxidation in aging and age-related diseases. Ann NY Acad Sci 2001; 928:22-38.
4. Cuervo AM, Bergamini E, Brunk UT, Droge W, Ffrench M, Terman A. Autophagy and aging: the importance of maintaining "clean" cells. Autophagy 2005; 1:131-40.
5. Hara T, Nakamura K, Matsui M, Yamamoto A, Nakahara Y, Suzuki-Migishima R, et al. Suppression of basal autophagy in neural cells causes neurodegenerative disease in mice. Nature 2006; 441:885-9.
6. Donati A, Cavallini G, Paradiso C, Vittorini S, Pollera M, Gori Z, et al. Age-related changes in the regulation of autophagic proteolysis in rat isolated hepatocytes. J Gerontol A Biol Sci Med Sci 2001; 56:288-93.
7. Vellai T. Autophagy genes and ageing. Cell Death Diff 2009; 16:94-102.
8. Simonsen A, Cumming R, Brech A, Isakson P, Schubert D, Finley K. Promoting basal levels of autophagy in the nervous system enhances longevity and oxidative stress in adult Drosophila. Autophagy 2008; 4:176-84.
9. Nakai A, Yamaguchi O, Takeda T, Higuchi Y, Hikoso S, Taniike M, et al. The role of autophagy in cardiomyocytes in the basal state and in response to hemodynamic stress. Nat Med 2007; 13:619-24.
10. Mizushima N, Yamamoto A, Hatano M, Kobayashi Y, Kabeya Y, Suzuki K, et al. Dissection of autophagosome formation using Apg5-deficient mouse embryonic stem cells. J Cell Biol 2001; 152:657-68.
11. Del Roso A, Vittorini S, Cavallini G, Donati A, Gori Z, Masini M, et al. Ageing-related changes in the in vivo function of rat liver macroautophagy and proteolysis. Exp Gerontol 2003; 38:519-27.
12. Terman A. The effect of age on formation and elimination of autophagic vacuoles in mouse hepatocytes. Gerontology 1995; 41:319-26.
13. Piantadosi CA, Carraway MS, Babiker A, Suliman HB. Heme oxygenase-1 regulates cardiac mitochondrial biogenesis via Nrf2-mediated transcriptional control of nuclear respiratory factor-1. Circ Res 2008; 103:1232-40.
14. Nishida Y, Arakawa S, Fujitani K, Yamaguchi H, Mizuta T, Kanaseki T, et al. Discovery of Atg5/Atg7-independent alternative macroautophagy. Nature 2009; 461:654-8.
15. Twig G, Elorza A, Molina AJ, Mohamed H, Wikstrom JD, Walzer G, et al. Fission and selective fusion govern mitochondrial segregation and elimination by autophagy. EMBO J 2008; 27:433-46.
16. Cook AR, Bardswell SC, Pretheshan S, Dighe K, Kanaganayagam GS, Jabr RI, et al. Paradoxical resistance to myocardial ischemia and age-related cardiomyopathy in NHE1 transgenic mice: A role for ER stress? J Mol Cell Cardiol 2009; 46:225-33.
17. Coleman R, Silbermann M, Gershon D, Reznick AZ. Giant mitochondria in the myocardium of aging and endurance-trained mice. Gerontology 1987; 33:34-9.
18. Terman A, Dalen H, Eaton JW, Neuzil J, Brunk UT. Mitochondrial recycling and aging of cardiac myocytes: the role of autophagocytosis. Exp Gerontol 2003; 38:863-76.
19. Scherz-Shouval R, Elazar Z. ROS, mitochondria and the regulation of autophagy. Trends Cell Biol 2007; 17:422-7.
20. Lopez Farre A, Casado S. Heart failure, redox alterations and endothelial dysfunction. Hypertension 2001; 38:1400-5.
21. Giordano FJ. Oxygen, oxidative stress, hypoxia and heart failure. J Clin Invest 2005; 115:500-8.
22. Nojiri H, Shimizu T, Funakoshi M, Yamaguchi O, Zhou H, Kawakami S, et al. Oxidative stress causes heart failure with impaired mitochondrial respiration. J Biol Chem 2006; 281:33789-801.
23. Prieura A, Peeper DS. Cellular senescence in vivo: a barrier to tumorigenesis. Curr Opin Cell Biol 2008; 20:150-5.
24. Yamaguchi O, Watanabe T, Nishida K, Kashiwase K, Higuchi Y, Takeda T, et al. Cardiac-specific disruption of the c-raf-1 gene induces cardiac dysfunction and apoptosis. J Clin Invest 2004; 114:937-43.
25. Kabeya Y, Mizushima N, Ueno T, Yamamoto A, Kirisako T, Noda T, et al. LC3, a mammalian homologue of yeast Apg8p, is localized in autophagosome membranes after processing. EMBO J 2000; 19:5720-8.
26. Trounce IA, Kim YL, Jun AS, Wallace DC. Assessment of mitochondrial oxidative phosphorylation in patient muscle biopsies, lymphoblasts and transmitochondrial cell lines. Methods Enzymol 1996; 264:484-509.

A Case of Localized IgG4-Related Thoracic Periarteritis and Recurrent Nerve Palsy

Masao Takahashi, MD, Takashi Shimizu, MD, Tsukasa Inajima, MD, Yumiko Hosoya, MD, Norifumi Takeda, MD, Nobukazu Ishizaka, MD, Hiroshi Yamashita, MD, Yasunobu Hirata, MD and Ryozo Nagai, MD

Abstract: Periarteritis, including periaortitis, is a systemic disorder characterized by an excessive fibroinflammatory reaction that can result in the compromise of great vessels and periarterial/periaortic structures. Recent studies have suggested that IgG4-related inflammation may play a role in chronic periaortitis. These pathologic conditions might represent a systemic disorder with fibrotic reaction rather than local inflammation. In this report, the authors describe a case of a 31-year-old man with marked periaortic fibrous thickening localized to the aortic arch, which was histologically and serologically proven to be IgG4 related. Positron emission tomography showed increased ^{18}F-fluorodeoxyglucose uptake at this region. Histologic examination revealed infiltration of lymphoplasmacytes and marked fibrosis with numerous IgG4-positive plasma cells. The serum concentration of IgG4 was 263 mg/dL. The size of the periaortic mass and ^{18}F-fluorodeoxyglucose uptake at this region markedly decreased under corticosteroid therapy. This case suggests that IgG4-related periarteritis can also occur as a solitary focus in the cardiovascular system.

Key Indexing Terms: Periarteritis; Periaortitis; IgG4-related sclerosing disease. **[Am J Med Sci 2011;341(2):166–169.]**

Chronic periarteritis and periaortitis are a part of a spectrum of idiopathic diseases characterized by fibroinflammatory reaction surrounding the arteries and the aorta. Chronic periaortitis includes idiopathic retroperitoneal fibrosis and inflammatory abdominal aortic aneurysm, and it is considered as a systemic disorder caused by the extended involvement of the aorta and raised inflammatory markers.[1] On the other hand, IgG (immunoglobulin G) 4-related sclerosing disease is also known as a systemic disorder of protean manifestations that may involve the pancreas,[2] retroperitoneum,[3] bile duct[4] and salivary glands.[5] It has been recently suggested that IgG4-related sclerosing disease may be linked to chronic periarteritis and that these 2 disorders might overlap, at least in part.[1] We encountered a case of IgG4-related periarteritis at the thoracic aortic arch without evidence of other organ involvement.

CASE REPORT

A 31-year-old Japanese man was admitted to our hospital because of an episode of hoarseness with no previous history of any serious disease. He had not been prescribed any medication. He was a current smoker. On physical examination, blood pressure was 116/70 mm Hg, and other vital signs were within normal range. His left vocal cord was paralyzed because of recurrent laryngeal nerve paralysis. A chest radiograph showed abnormal protrusion of the aortic arch (Figure 1A), and computed tomography (CT) revealed a mass surrounding the aorta at its bifurcation to the subclavian artery (Figure 1B). ^{18}F-fluorodeoxyglucose (^{18}F-FDG) positron emission tomography (PET) showed increased tracer uptake at the aortic arch with no abnormal tracer uptake in other regions (Figure 1C). The following laboratory data were obtained: serum C-reactive protein, 0.62 mg/dL; erythrocyte sedimentation rate, 41 mm/hr; IgG, 1884 mg/dL; IgG4, 263 mg/dL; serum soluble interleukin-2 receptor, 458 U/mL; and absence of detectable antinuclear antibodies. IgG4 subtype accounted for 14.0% of the IgG fraction. CT and magnetic resonance imaging showed no abnormality in the lymph nodes, pancreas or retroperitoneum. Histologic analysis of the thoracoscopic biopsy specimen of the mass at the aortic arch demonstrated diffuse infiltration of lymphoplasmacytes and marked fibrosis, with no significantly atypical cells (Figures 2A and 2B).

Immunostaining for CD3 and CD20 showed that the lymphocytes were polyclonal and included mainly CD20-positive B cells and CD3-positive T cells. The number of CD20-positive B cells was larger than that of CD3-positive T cells (Figures 3A and 3B). In addition, immunostaining for IgG4 revealed many IgG4-positive plasma cells within the lesion (Figure 3C). On the basis of these findings, we made the pathologic diagnosis of IgG4-related periarteritis localized to the aortic arch. IgG4-positive disease frequently accompanies sclerosing pancreatitis. However, magnetic resonance cholangiopancreatography showed that in this patient, the pancreatic duct and bile duct were intact. No finding characteristic of sclerosing pancreatitis was observed. Consequently, we treated him with 40 mg of prednisolone daily for localized IgG4-related periarteritis. Eight weeks later, hoarseness was found to have gradually ameliorated, the chest radiograph and CT scan revealed improvement of the periaortic mass (Figures 4A and 4B), abnormal ^{18}F-FDG uptake of the aorta on PET scanning was reduced (Figure 4C) and all laboratory data were within normal range. We tapered the dose of prednisolone to 5 mg, and no signs of recurrence have been observed during the follow-up examinations (1 year).

DISCUSSION

IgG4-related sclerosing disease was first reported as sclerosing pancreatitis.[2] Since then, patients with histologically proven IgG4-positive plasma cell infiltration and/or markedly elevated serum IgG4 levels are being increasingly diagnosed. These abnormal findings lead to the development of IgG4-related diseases, which may affect different organs or tissues such as the bile duct, the salivary glands and the retroperito-

From the Department of Cardiovascular Medicine (MT, TS, TI, YII, NT, NI, HY, YH, RN), Graduate School of Medicine, The University of Tokyo, Hongo, Bunkyo-ku, Tokyo, Japan; and Division of Cardiology (NI), Department of Internal Medicine III, Osaka Medical College, Daigaku-machi, Takatsuki-shi, Osaka, Japan.

Submitted July 30, 2010; accepted in revised form September 9, 2010.

Correspondence: Masao Takahashi, MD, PhD, Department of Cardiovascular Medicine, Graduate School of Medicine, The University of Tokyo, Hongo 7-3-1, Bunkyo-ku, Tokyo 113-8655, Japan (E-mail: masaotakahashi-gi@umin.ac.jp).

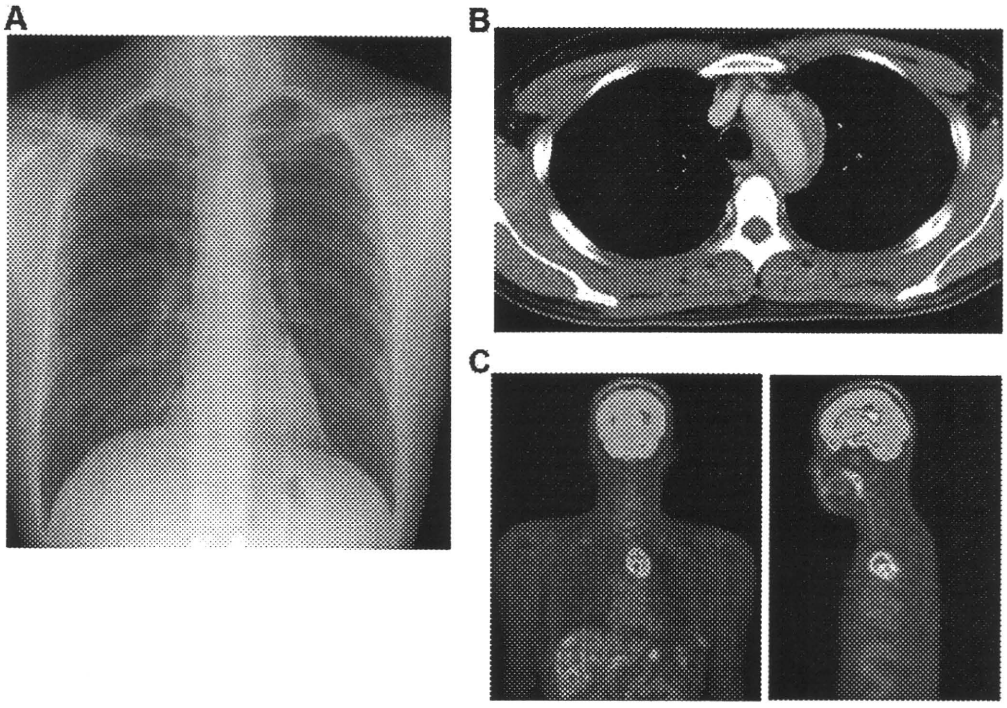

FIGURE 1. Before the corticosteroid therapy, the chest radiograph (A) showed an abnormal protrusion of the aortic arch, contrast medium-enhanced CT (B) of the chest revealed a periaortic mass in the mediastinum and ^{18}F-FDG-PET (C) showed increased tracer uptake at the aortic arch.

neum. Chronic periaortitis is characterized as a fibroinflammatory reaction usually affecting the abdominal aorta. Although the clinical spectrum of chronic periarteritis or periaortitis has not been well defined, retroperitoneal fibrosis and inflammatory abdominal aortic aneurysm are considered to belong to this entity.[1] Of note, there is an increasing body of evidence showing that chronic periaortitis is a feature of IgG4-related sclerosing diseases. For example, in retroperitoneal fibrosis, thickened fibrotic tissue is characterized by diffuse infiltration of IgG4-positive plasma cells.[6] Moreover, IgG4-related diseases can occur not only in tissues near the aorta but also in the wall of arteries including coronary arteries.[7] Therefore, periarteritis is an entity similar to periaortitis.

Although in most cases, the abdominal aorta and neighboring structures are affected, in few cases, only the thoracic aorta is involved.[8,9] One of the reported cases showed not only fibrosis of the thoracic aorta but also retroperitoneal fibrosis with raised IgG4 levels and involvement of other organs.[8] Another patient had an IgG4-related inflammatory aneurysm of the aortic arch whose maximum diameter was 55 mm.[9] In contrast to these 2 cases, no evidence of other organ involvement or of aneurysmal change of the aorta was found in our patient.

It has been suggested that chronic periarteritis and IgG4-related sclerosing disease might represent a systemic inflammatory disorder rather than local inflammatory disease, because each is characterized by constitutional symptoms and raised inflammatory markers with extended involvement of the aorta.[10] However, in our patient, the inflammatory reaction was restricted to the surrounding tissue of the aortic arch, and no abnormal involvement of other organs was detected. The mechanism of solitary and localized involvement in our patient remains to be identified. Some investigators have suggested that local inflammatory reaction to oxidized low-density lipoproteins and ceroids in the atherosclerotic plaques might cause periarteritis.[11] Our patient was a young man with few risk factors for atherosclerosis except for smoking. No atherosclerotic plaque was found in the biopsy specimen.

A recent study reported that T-helper 2 (T_H2) cells and regulatory immune reactions are upregulated in tissues affected by

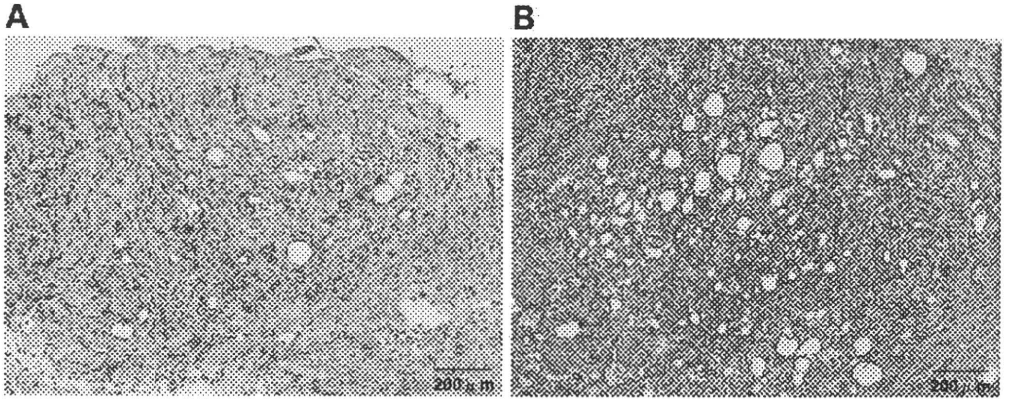

FIGURE 2. Histopathologic findings of the periaortic mass biopsy specimen. Hematoxylin and eosin staining showed lymphoplasmacytic infiltration intermixed with irregular fibrosis (A). Elastic van Gieson stain revealed marked fibrosis (B).

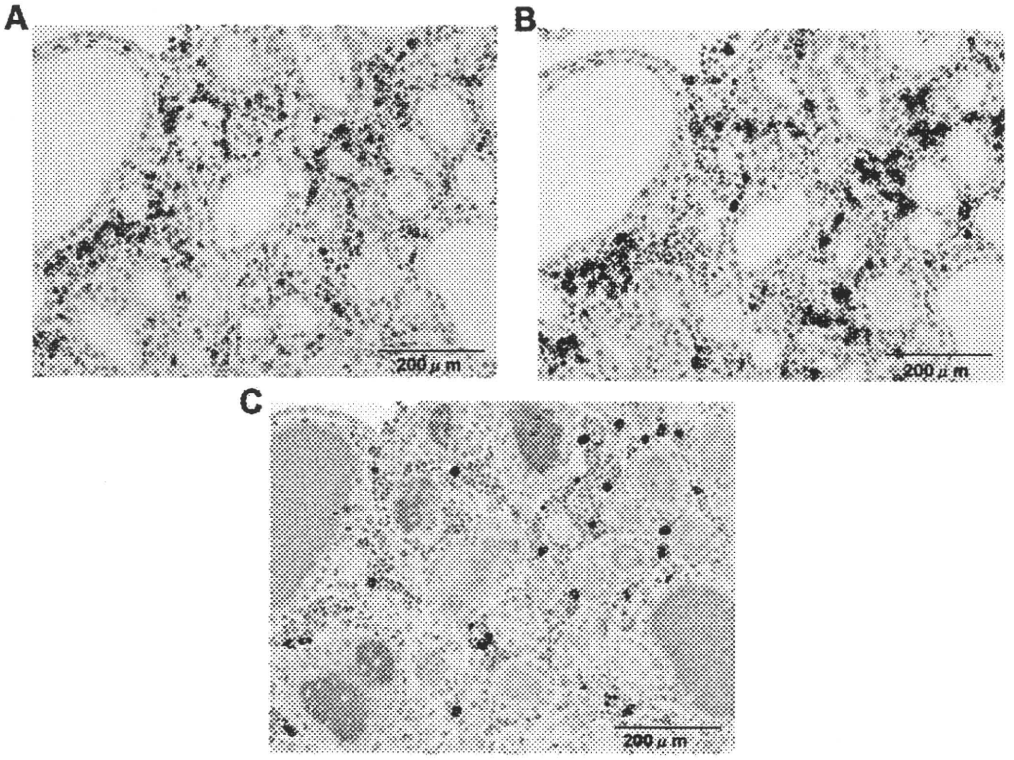

FIGURE 3. Immunostaining of the biopsy specimen for CD3 (A) and CD20 (B) showed that the infiltrate included mainly CD20-positive B cells and CD3-positive T cells. Immunostaining for IgG4 revealed many IgG4-positive plasma cells within the lesion (C).

IgG4-related sclerosing disease,[12] suggesting the involvement of T_H2 cell-mediated immune reaction in the pathogenesis of this disorder. Nevertheless, we did not evaluate the activity of T_H2-associated cytokines before corticosteroid therapy in our patient.

CT revealed a periaortic mass surrounding the aortic arch at a narrow region, and ^{18}F-FDG-PET disclosed remarkably localized tracer uptake. According to these findings, other diseases such as malignant lymphoma should be ruled out. Soluble interleukin-2 receptor level was found to be within normal range (458 U/mL), and serum IgG4 was elevated (263 mg/dL). Although these findings may not be characteristic of a malignant tumor,[6] pathologic examination was considered cru-

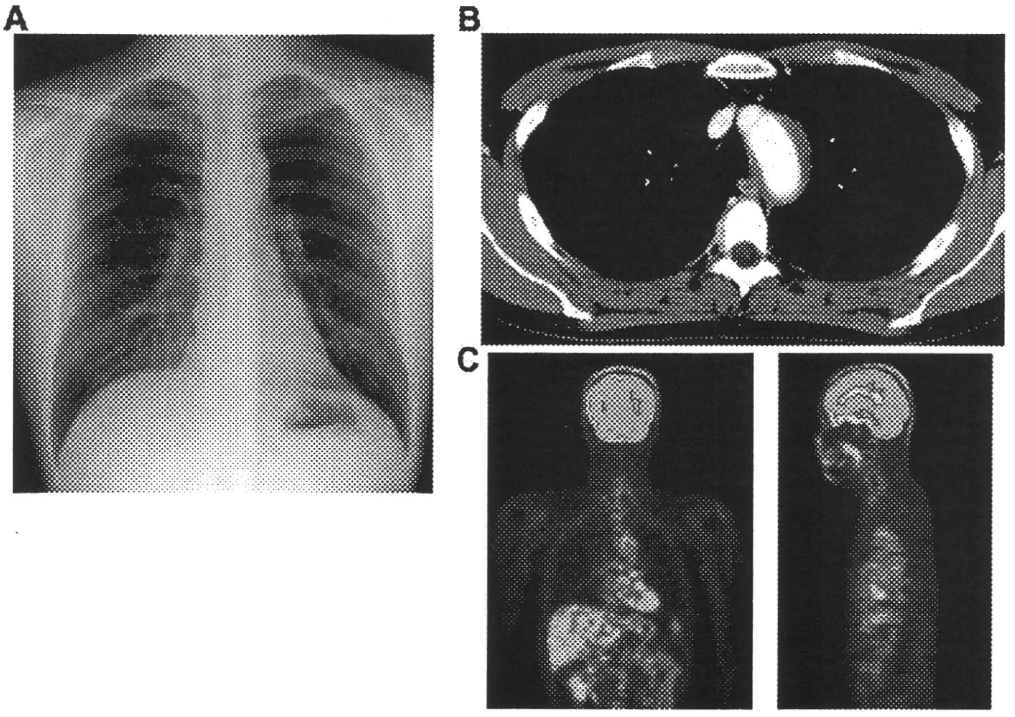

FIGURE 4. After the corticosteroid therapy, the chest radiograph (A) and CT scan (B) revealed a decrease in size of the periaortic mass. PET scanning (C) revealed no abnormal uptake of ^{18}F-FDG at the aortic arch.

cial for the differential diagnosis. Presence of the diffuse infiltration of the IgG4-positive lymphoplasmacytic cells without the evidence of atypicality was useful in distinguishing IgG4-related periarteritis from malignant lymphoma in our case. Serum IgG4 is useful for the diagnosis and evaluation of IgG4-related periarteritis. ^{18}F-FDG-PET is not specific for the diagnosis of IgG4-related periarteritis or chronic periaortitis,[13] but it is useful to assess the progression of the disease and search for other abnormalities in the whole body.

In conclusion, we have presented a case with IgG4-related periarteritis localized to the thoracic aorta. After the induction of corticosteroid therapy, the size of the fibrous mass surrounding the aortic arch decreased, the enhanced uptake of ^{18}F-FDG also decreased and recurrent nerve palsy disappeared. In this patient, accurate diagnosis led to suitable treatment.

REFERENCES

1. **Palmisano A, Vaglio A.** Chronic periaortitis: a fibro-inflammatory disorder. Best Pract Res Clin Rheumatol 2009;23:339–53.
2. **Hamano H, Kawa S, Horiuchi A, et al.** High serum IgG4 concentrations in patients with sclerosing pancreatitis. N Engl J Med 2001;344: 732–8.
3. **Hamano H, Kawa S, Ochi Y, et al.** Hydronephrosis associated with retroperitoneal fibrosis and sclerosing pancreatitis. Lancet 2002;359: 1403–4.
4. **Hamano H, Kawa S, Uehara T, et al.** Immunoglobulin G4-related lymphoplasmacytic sclerosing cholangitis that mimics infiltrating hilar cholangiocarcinoma: part of a spectrum of autoimmune pancreatitis? Gastrointest Endosc 2005;62:152–7.
5. **Kitagawa S, Zen Y, Harada K, et al.** Abundant IgG4-positive plasma cell infiltration characterizes chronic sclerosing sialadenitis (Kuttner's tumor). Am J Surg Pathol 2005;29:783–91.
6. **Zen Y, Onodera M, Inoue D, et al.** Retroperitoneal fibrosis: a clinicopathologic study with respect to immunoglobulin G4. Am J Surg Pathol 2009;33:1833–9.
7. **Matsumoto Y, Kasashima S, Kawashima A, et al.** A case of multiple immunoglobulin G4-related periarteritis: a tumorous lesion of the coronary artery and abdominal aortic aneurysm. Hum Pathol 2008;39: 975–80.
8. **Zen Y, Sawazaki A, Miyayama S, et al.** A case of retroperitoneal and mediastinal fibrosis exhibiting elevated levels of IgG4 in the absence of sclerosing pancreatitis (autoimmune pancreatitis). Hum Pathol 2006; 37:239–43.
9. **Ishida M, Hotta M, Kushima R, et al.** IgG4-related inflammatory aneurysm of the aortic arch. Pathol Int 2009;59:269–73.
10. **Vaglio A, Corradi D, Manenti L, et al.** Evidence of autoimmunity in chronic periaortitis: a prospective study. Am J Med 2003;114:454–62.
11. **Vaglio A, Salvarani C, Buzio C.** Retroperitoneal fibrosis. Lancet 2006;367:241–51.
12. **Zen Y, Fujii T, Harada K, et al.** Th2 and regulatory immune reactions are increased in immunoglobin G4-related sclerosing pancreatitis and cholangitis. Hepatology 2007;45:1538–46.
13. **Pipitone N, Ghinoi A, Versari A, et al.** Images in cardiovascular medicine. Chronic periaortitis. Circulation 2008;118:1214–6.

RETRACTION

Respiratory Stress Response: A Novel Diagnostic Method for Detection of Significant Coronary Artery Disease From Finger Pulse Wave Analysis During Brief Respiratory Exercise: RETRACTION

The authors have informed us that the above article by Dr. Shiyovich et al published in *The American Journal of the Medical Sciences* contains results that were significantly biased. The authors continued investigating the above novel diagnostic test in additional studies in the target population – ambulatory patients referred to evaluate the presence of significant coronary artery disease and found much lower diagnostic efficacy. In cooperation with the developing company (SPIROCOR) the authors meticulously reanalyzed the above study results and found that the results of the new test were matched incorrectly with the gold standard (QCA) in a significant amount of cases, hence the results reported in the published article were significantly biased and not reliable. This incorrect matching is the subject of an ongoing investigation. Retrospectively, the authors believe it was nearly impossible to notice this incorrect matching at the time. Following these findings SPIROCOR is shutting down all clinical studies and activities. Importantly, the new test has not been implemented into clinical use anywhere in the world.

We are therefore retracting the paper by Dr. Shiyovich et al published in *The American Journal of the Medical Sciences.*

REFERENCE

Shiyovich A, Jafari J, Blaer Y, et al. Respiratory Stress Response: A Novel Diagnostic Method for Detection of Significant Coronary Artery Disease From Finger Pulse Wave Analysis During Brief Respiratory Exercise. Am J Med Sci 2010;339:440–7.